

## Fluid Substitution in Anisotropic Carbonates - I

*Naveen Gupta\* and Ravi Sharma*

*Department of Earth Sciences/Indian Institute of Technology Roorkee, India*

[Naveennjn1729@gmail.com](mailto:Naveennjn1729@gmail.com)

### Keywords

Anisotropy, Carbonates, Reservoir Characterization, Elastic Moduli, VTI

### Summary

The need to analyze subtle differences in seismic amplitude variation is gaining tremendous ground and so is the need to accurately model the medium that generates these subtle seismic signatures. The detection of the seismic response becomes more challenging when the medium is fractured. These fractures could be natural or artificial. Porous medium with embedded fractures in multiple orientation is quite common phenomena with natural reservoir, particularly in shales and carbonates. Gassmann isotropic relation is applicable only for homogeneously distributed equivalent porosity mediums. In natural reservoirs, particularly the fractured ones (orthorhombic medium), concept of equivalent porosity medium do not hold any more even though fractures occupy very little porosity volume in the background porous media, their compliance in a stress system with a saturant type could no longer be a straight forward problem to predict the seismic response of such fluid filled systems. In this work, we explore the possibility of detecting the nature of anisotropy in the given rock by comparing the equivalent porosity distribution through Gassmann isotropic and Gassmann anisotropic prediction. We found that consideration of a VTI medium does not make any difference in the predicted values of seismic velocity and modulus.

### Introduction

Seismic amplitude analysis constitutes a major part of exploration and feasibility studies in oil and gas reservoirs assisting in recovery improvement. Rock physics models have been widely used to establish relationships between measured seismic amplitudes and the rock and fluid properties resulting those

amplitudes. This relationship is easy to establish if the material obeys Gassmann assumption (Gassmann, 1951). For the material deviating from Gassmann behavior, customized algorithms and work flows have been produced over the years now for solving saturated response of the media at the insitu conditions (O'Connell and Budiansky, 1977; Thomsen, 1986 & 1995; Schoenberg and Sayers 1995; Hudson, 2000 & 2001; Gurevich, 2002; Wang, 2002; Mavko and Bandhopadhyay, 2009; Sil et al. 2011; Huang et al. 2013 & 2014). In this series

From the geological understanding of the sedimentary rock sequences, we understand that most complex system to deviate from Gassmann behavior would need to exhibit heterogeneous and anisotropic (fractured) tendencies in measured values. In this series naturally fractured reservoirs have attracted lot of interest in exploration and production over the last decade or so. The elastic properties of fluid saturated porous media fractures can be studied using equations of anisotropic poroelasticity. When the fractures are aligned (Figure 1), it represents a particular case of a transversely isotropic (TI) porous medium. The five elastic constants of the resultant TI medium are derived as a function of dry isotropic background porous matrix, the fracture, and fluid bulk modulus (Wang, 2002; Gurevich, 2003). More general relationships between dry and fluid-saturated properties of fractured porous media can be based on the general linear-slip model of the medium with parallel fractures (Schoenberg and Douma, 1988; Schoenberg and Sayers, 1995). This model accounts for excess compliance due to the presence of fractures, and requires no assumptions about the microstructure or microgeometry of the fractures.

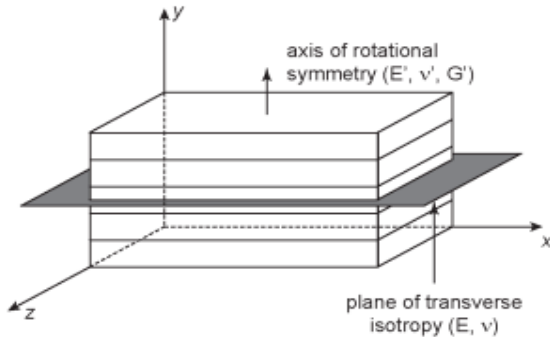


Figure 1 Cartoon showing Vertically Transverse Isotropic (VTI) media

Carbonate rocks are known to exhibit both heterogeneous and anisotropic texture (Sharma et al. 2013). In this paper, we identified a set of literature data (Wang, 2002) that had the lab measured six stiffness coefficients ( $C_{11}$   $C_{33}$   $C_{44}$   $C_{13}$   $C_{66}$   $C_{12}$ ) for transverse anisotropy (TI) case at two different stresses (6.90 MPa and 55.17 MPa) in the limestone formations of Canada. The dominant mineral is calcite. The porosity ranges from 0.6% to 16%. The constants used for calculating various reservoir values are listed at table 1.

**Table 1** Elastic constants and density applied in present study (Sharma et al. 2006).

Mineral / Fluid	Bulk Modulus (GPa)	Shear Modulus (GPa)	Density (Kg/m <sup>3</sup> )
Calcite	75	31	2710
Water	2.25	0	1000
Brine	2.94	0	1030

The objective is to exploit the idea of saturation in equivalent porosity medium rock and compare the calculated elastic moduli; 1) using Gassmann isotropic model considering the porosity is homogenous and isotropic and 2) Gassmann anisotropic model considering the same porosity is distributed in transversely isotropic planes. If the rock is indeed anisotropic the two response would be different. We used data sets at two pressure points on the samples listed in Wang (2002). We presumed that the sample with fracture discontinuity would show large compliance and therefore large change in

velocity and moduli values with respect to the low pressure samples. For fluid substitution problems in such anisotropic rocks, many methods have been proposed. In this work, we used Gurevich (2003) to derive fluid substitution relations for VTI media. The equations derive are general for any elastic, isotropic rocks with vertical fracture sets. This work is the first stage before we attempt to model the effective elastic response for a full orthorhombic rock using laboratory measured data.

**Method**

For isotropic porous reservoirs, the effect of fluid properties on seismic characteristics is expressed through Gassmann’s relation (Equation 1).

$$K_{sat} = K_{frame} + \frac{\left(1 - \frac{K_{frame}}{K_{matrix}}\right)^2}{\frac{\phi}{K_f} + \frac{(1-\phi)}{K_{matrix}} - \frac{K_{frame}}{K_{matrix}^2}} \dots\dots\dots(1)$$

Where  $K_{sat}$ ,  $K_{frame}$ ,  $K_{matrix}$  and  $K_f$  are the bulk moduli of the saturated rock, porous rock frame, mineral matrix and pore fluid respectively and  $\phi$  is the porosity (as fraction) of model, shear modulus is considered independent of the pore fluid and held constant during the fluid substitution. But the application of the model is limited in heterogeneous and anisotropic reservoir.

For the anisotropic medium, the stiffness tensor of dry rock skeleton and the saturated rock are related as (Gurevich, 2003);

$$C_{ij}^{sat} = C_{ij}^0 + \alpha_i \alpha_j M, \quad i, j = 1, \dots, 6 \dots\dots\dots(2)$$

Where

$$\alpha_m = 1 - \frac{\sum_{n=1}^3 C_{mn}^0}{3K_{matrix}} \dots\dots\dots(3)$$

For  $m=1,2$  and  $3$ ,  $\alpha_4, \alpha_5, \alpha_6=0$  and

$$M = \frac{K_{matrix}}{\left(1 - \frac{K^*}{K_{matrix}}\right) - \phi \left(1 - \frac{K_{matrix}}{K_f}\right)} \dots\dots\dots(4)$$

In Eq. (4)  $\phi$  is the overall porosity of the fractured rock i.e. sum of primary and secondary porosity and  $K^*$  denotes generalized drain bulk modulus, which is defined as

$$K^* = \frac{1}{9} \sum_{i=1}^3 \sum_{j=1}^3 C_{ij}^0 \quad \dots\dots\dots(5)$$

From Eq. (2) we see that Gassmann's anisotropic equation requires stiffness tensors of the dry rock skeleton. We seldom have enough measurements to calculate it for the general anisotropic media. Therefore, we consider two cases: (1) rocks composed of isotropic matrix embedded by a set of vertical or horizontal invariant fractures i.e. VTI or HTI medium. (2) both vertical and horizontal invariant fractures embedded in the background isotropic matrix (orthorhombic medium). The isotropic rocks are characterized by the Lamé parameters ( $\lambda$ ) and shear modulus ( $\mu$ ) and the embedded fractures are characterized by the dimensionless normal and tangential fracture weakness,  $\Delta_N$  and  $\Delta_T$ , respectively. The stiffness tensor of dry rock for transverse isotropic (TI) model can be expressed as:

$$C_{ij} = \begin{pmatrix} C_1 & 0 \\ 0 & C_2 \end{pmatrix} \quad \dots\dots\dots(6)$$

$$C_1 = \begin{pmatrix} c_{11} & c_{12} & c_{13} \\ c_{12} & c_{11} & c_{13} \\ c_{13} & c_{13} & c_{33} \end{pmatrix} \quad \dots\dots\dots(7)$$

$$C_2 = \begin{pmatrix} c_{44} & 0 & 0 \\ 0 & c_{44} & 0 \\ 0 & 0 & c_{66} \end{pmatrix} \quad \dots\dots\dots(8)$$

Where

$$C_1 = \begin{pmatrix} M(1 - \Delta_N) & \lambda(1 - \Delta_N) & \lambda(1 - \Delta_N) \\ \lambda(1 - \Delta_N) & M(1 - \Delta_N) & \lambda(1 - \Delta_N) \\ \lambda(1 - \Delta_N) & \lambda(1 - \Delta_N) & M(1 - r^2 \Delta_N) \end{pmatrix} \dots\dots(9)$$

$$C_2 = \begin{pmatrix} \mu & 0 & 0 \\ 0 & \mu & 0 \\ 0 & 0 & \mu(1 - \Delta_T) \end{pmatrix} \quad \dots\dots\dots(10)$$

$$\Delta_N = \frac{\epsilon(\lambda+2\mu)^2}{\epsilon(\lambda+2\mu)^2 + 2\mu(\lambda+\mu)} \quad \dots\dots\dots(11)$$

$$\Delta_T = \frac{2\gamma}{1+2\gamma} \quad \dots\dots\dots(12)$$

$$M = (\lambda + 2\mu) \quad \dots\dots\dots(13)$$

$$r = \frac{\lambda}{(\lambda+2\mu)} \quad \dots\dots\dots(14)$$

In the above equations  $\epsilon$  and  $\gamma$  are the Thomsen's parameters. If the stiffness tensor of dry rock is known then Eq. (2) to Eq. (5) can be used to calculate the stiffness tensor of saturated rock otherwise Thomsen's parameters are required for the computation of stiffness tensor of dry rock as described from Eq. (6) to Eq. (14).

### Results

Overall porosity in these samples vary from 1% to 16%. From the conventional understanding, generally the low porosity rocks would lead to a stiffer (low porosity, high velocity) dry frame. However, if the same low porosity were to be distributed among fractures, the dry frame would be much compliant to the applied stress. Assuming that fractures are aligned in horizontal planes (Figure 1), we examined the results of Gassmann isotropic and Gassmann anisotropic model using the data in Wang (2002). Given a reasonable match of the measured and the Gassmann isotropic predicted compressive and shear-wave velocities (Figure 2), we went on to compare the Gassmann isotropic and with the anisotropic values for anisotropy effects on elastic parameters of a saturated VTI rock.

Double click here to type your header

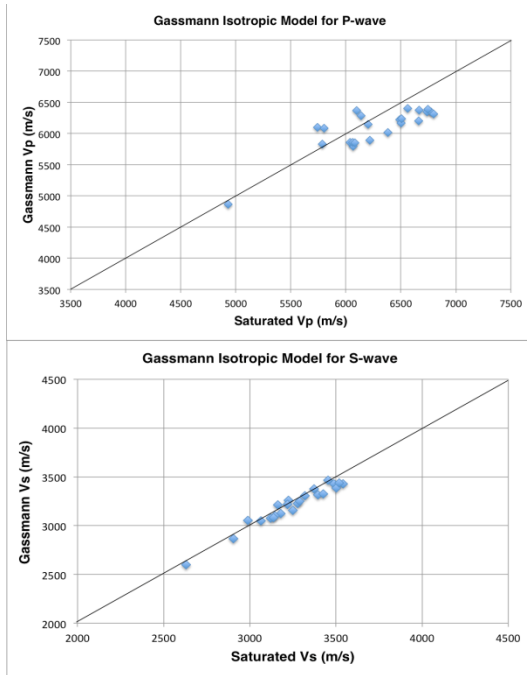


Figure 2 (a) Measured P-wave velocity versus Gassmann's (isotropic) values and (b) measured S-wave velocity versus Gassmann's (isotropic) values (Sharma et al. 2006).

We used Lamé parameters ( $\lambda$ ) and shear modulus ( $\mu$ ) for characterizing the embedded fractures by using the dimensionless normal and tangential fracture weakness,  $\Delta_N$  and  $\Delta_T$ , respectively. Figure 3a and 3b shows the predicted Vp and Vs values for isotropic and the anisotropic models. The isotropic values are marginally over predicted for both the pressure values (6.90 MPa and 55.17 MPa), particularly for the higher porosity samples. The increase in pressure has resulted in significant jump of  $\sim 50\%$  in the Vp values and  $\sim 10\%$  the Vs values. This jump is more evident in the higher porosity samples and much less in low porosity samples. This behavior of Vp and Vs velocities clearly indicates that the samples had a concentration of fractures in various planes that affected the Vp much more than the Vs with increases in pressure. So long the compliance from the fractures was available, isotropic and the anisotropic model did not converge on the line of equal values but the moment the compliance was gone, the data from the two models was exactly lying on the equal value line

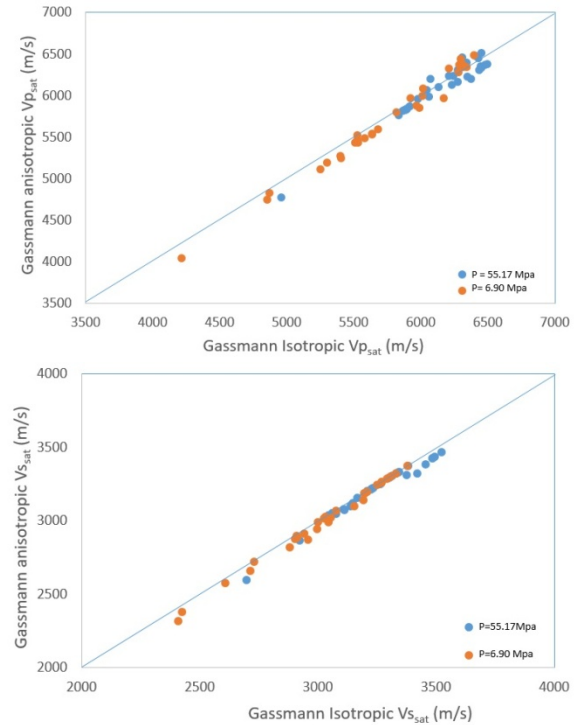


Figure 3 Comparative analysis of Gassmann isotropic with Gassmann anisotropic for (a) compressive-wave velocity and (b) shear-wave velocity.

As velocities carry the combined effect of bulk and shear moduli, we investigated the impact of change in pressure and the predictions from the two models on elastic moduli values. Similar to Vp values, Figure 4a shows that for higher porosity values (higher compliance from the pores), the anisotropic model under predicts the bulk moduli but for lower porosity samples (less compliance available), the bulk moduli values are concentrated around the line of equal values. This observation is particularly true for the low pressure stage. With increase in pressure (no compliance available), the two models converge within the admissible error. For the shear modulus in Figure 4b, as intuitive, the impact of compliant pores on the shear modulus is not that prominent. The figure shows increased values of shear moduli with increase in overburden pressure.

Double click here to type your header

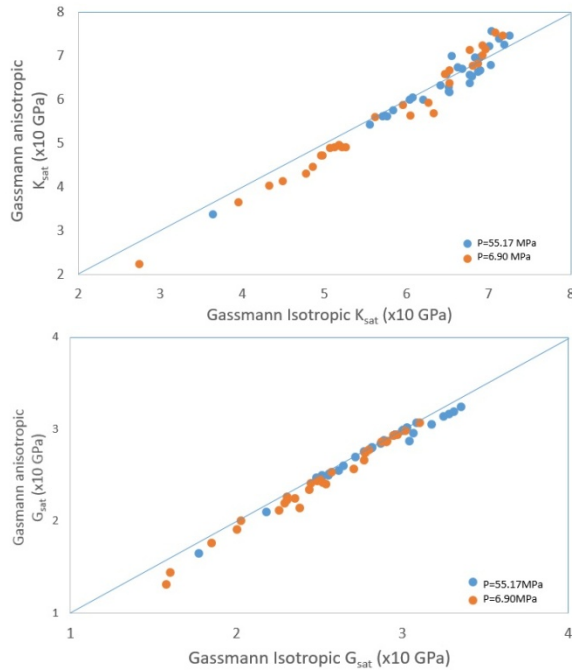


Figure 4 Comparative analysis of Gassmann isotropic with Gassmann anisotropic for (a) bulk modulus and (b) shear modulus.

In the end, we plotted Gassmann anisotropic moduli and measured moduli versus porosity (Figure 5). For very low and high porosity values, bulk moduli shows similar values as that of measured values. However, for the porosity in between the Gassmann anisotropic model mostly underpredicted the values. For the shear modulus we observe that except for the high pressure measured data, the other three values plots around same value of shear modulus. Hence the high pressure values of 55.17 MPa, caused drastic changes in the matrix, causing its rigidity to increase multifold. Such samples, particularly for the shear modulus values may surprise and be very separate from the field observation that exist over the entire porosity range.

### Conclusion

Samples under varying pressures, it is concluded that sample have fractured planes of anisotropy of the VTI form. Using data from two pressure stages, we found that higher pressure clearly shows affect of compliant pores on moduli and velocity, particularly in the higher porosity values. Gassmann anisotropic

model underpredicts the velocity and moduli values with respect to the Gassmann isotropic model. For the low porosity values, both Gassmann isotropic and Gassmann anisotropic models show converging values at both pressure stages. The under-predicted moduli in carbonates is partly due to the violation of constant shear modulus at different fluids. Particularly for low porosity rocks, the fluid rock interaction is hard to understand and so is the under prediction of data.

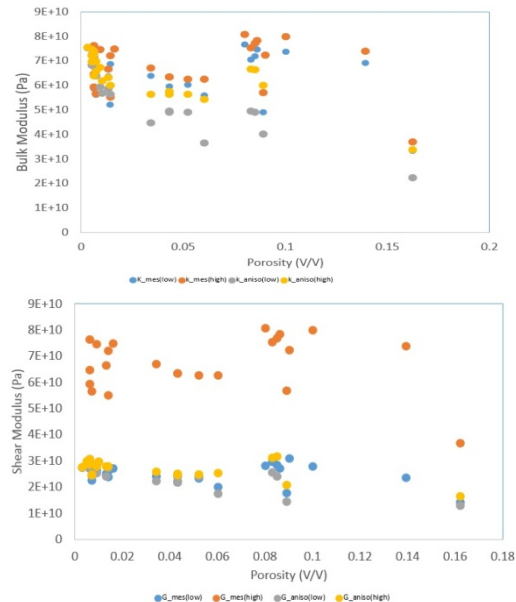


Figure 5 Comparative analysis of Gassmann anisotropic and measured values of (a) bulk modulus and (b) shear modulus at two different pressures

### References

- Gurevich, B., 2003, Elastic properties of saturated porous rocks with aligned fractures, *J. Appl. Geophys.*, 54(3–4), 203–218.
- Hudson, J. A., 2000, The effect of fluid pressure on wave speeds in a cracked solid, *Geophys. J. Int.*, 143(2), 302–310.
- Thomsen, L., 1986, Weak elastic anisotropy, *Geophysics*, 51(10), 1954–1966.
- Thomsen, L., 1995, Elastic anisotropy due to aligned cracks in porous rock, *Geophys. Prospect.*, 43(6), 805–829.

**Double click here to type your header**

Wang, Z., 2002, Seismic anisotropy in sedimentary rocks, Part 2: Laboratory data: *Geophysics*, 67, 1423–1422.

Huang, L., Jiang, T., Omoboya, B., Dyaur, N., Stewart, R. R., and Sil, S., 2013, Fluid substitution for an HTI medium, *SEG Technical Program Expanded Abstracts*, 516, 2659–2663.

Huang, L., Stewart, R. R., Sil, S., and Dyaur, N., 2014, Fluid substitution effects on seismic anisotropy, *SEG Technical Program Expanded Abstracts*, 64, 330–335.

Mavko, G., Mukerji, T., and Dvorkin, J., 2009, *The Rock Physics Handbook*, Cambridge University Press, April 2009.

O’Connell, R. J., and Budiansky, B., 1977, Viscoelastic properties of fluid-saturated cracked solids, *J. Geophys. Res.*, 82(36), 5719–5735.

Schoenberg, M., and Douma, J., 1988, Elastic wave propagation in media with parallel fractures and aligned cracks, *Geophys. Prospect.*, 36(6), 571–590.

Schoenberg, M., and Sayers, C., 1995, Seismic anisotropy of fractured rock, *Geophysics*, 60(1), 204–211.

Sil, S., Sen, M., and Gurevich, B., 2011, Analysis of fluid substitution in a porous and fractured medium, *Geophysics*, 76(3), WA157–WA166.

Sharma R., Prasad M., Batzle M., Vega s., 2013, Sensitivity of flow and elastic properties to fabric heterogeneity in carbonates: *Geophysical Prospecting*, 2013, 61, 270–286.

#### **Acknowledgement**

We thank Dr. Manika Prasad for her kind support and inputs in interpreting the original dataset, which this is based on.

